JOURNAL OF SOLID STATE CHEMISTRY 53, 313–322 (1984)

A Mössbauer Study of $Fe_2P_{1-x}Si_x$ ($x \leq 0.35$)

PER JERNBERG, A. A. YOUSIF,* LENNART HÄGGSTRÖM, AND YVONNE ANDERSSON†

Institute of Physics, Uppsala University, Box 530, and †Institute of Chemistry, Uppsala University, Box 531, S-751 21 Uppsala, Sweden

Received November 28, 1983; in revised form February 27, 1984

A crystallographic hexagonal/orthorhombic transformation is observed in partially Si-substituted Fe_2P. The transformation temperature dependence is shown to increase linearly with increasing P/Si substitution. The paramagnetic/ferromagnetic transition temperature is also found to increase with increasing substitution, e.g., $T_c = 216$ K for $x = 0$ and $T_c = 660$ K for $x = 0.35$. In the hexagonal phase the P/Si substitution is shown to be close to random with respect to the two phosphorus sites. It has been possible from the ^{57}Fe Mössbauer spectra to distinguish between iron sites having zero or one silicon nearest neighbor at either of the phosphorus sites. In the orthorhombic phase, the Mössbauer spectra were very complex and since complete crystal data are not yet available, only limited information can be drawn from these spectra.

1. Introduction

There have been several studies of Fe_2P and of substitutional solid solutions of different elements in Fe_2P during the last 2 decades. Summaries of available information from these studies are given by Chandra *et al.* (*1*) and by Ericsson *et al.* (*2*). Pure stoichiometric Fe_2P, for example, exhibits a first-order para-ferromagnetic transition at ~216 K with a saturation magnetic moment in the ferromagnetic state of 1.46 μ_B per iron atom. The moments are directed along the hexagonal *c*-axis. The Curie temperature and the type of transition have been found to be very sensitive to the presence of vacancies and impurity atoms (*3*). The substitution of anions in hexagonal Fe_2P have been examined by Catalano *et al.* (*4*). They found that the Fe_2P-type of structure was retained and that the unit cell volume increased monotonically with increasing As substitution. The observed magnetic properties, e.g., increase in T_c and saturation moments with x, were interpreted on the basis of the Stoner model for itinerant magnetism. Furthermore, the P/As substitution was found to take place preferentially on the P(1) site. For $Fe_2P_{1-x}B_x$ with $x \leq 0.15$ a Mössbauer and X-ray study was performed by Chandra *et al.* (*1*). The Fe_2P-type structure was retained also in this case but traces of other phases were present for $x = 0.15$, indicating a boron content in slight excess of the $Fe_2P_{1-x}B_x$ solubility limit. The magnetic ordering temperature increased rapidly with increasing boron

* On leave from Sudan Atomic Energy Commission, Khartoum, Sudan.

0022-4596/84 $3.00

content and it was possible from the Mössbauer spectra to distinguish between iron atoms having zero or one boron atoms in its immediate environment. The boron atoms were also found to substitute preferentially for phosphorus at the singlefold P(2) site in the Fe_2P structure in contrast to the P(1)/As substitution described above.

These preferential substitutions can be explained by the size factor argument put forward by Rundqvist (*5*). He proposed that atoms having larger radius than P (e.g., As and Si) should preferentially occupy the P(1) site while atoms of smaller radius (e.g., *B*) should occupy the P(2) site. In order to test this idea further, this Mössbauer study of the system $Fe_2P_{1-x}Si_x$ was performed.

2. Sample Preparation and Structure Data

Master alloys of composition Fe_2P, $Fe_2P_{0.75}Si_{0.25}$, and $Fe_2P_{0.33}Si_{0.67}$ were synthesized from high purity elements in an induction furnace. Alloys of different compositions were prepared by sintering appropriate mixtures of the master alloys in evacuated silica tubes at 1270 K. The products were examined by X-ray powder diffraction at room temperature in focusing Hägg–Guinier-type cameras, and the following results were obtained.

A substitutional solid solution of silicon in the hexagonal Fe_2P phase occurs up to a limiting composition of $Fe_2P_{0.83}Si_{0.17}$ at room temperature. The unit cell dimensions obtained for $Fe_2P_{0.90}Si_{0.10}$ were a = 5.9212(2) Å and c = 3.4226(3) Å, which can be compared with 5.8675 and 3.4581 Å, respectively, for Fe_2P. At higher silicon contents a new ternary phase is formed. This phase is homogeneous in the range $Fe_2P_{1-x}Si_x$, $0.20 < x < 0.36$, judging from alloys annealed at 1270 K. The room temperature powder diffraction lines can be indexed on a body-centered orthorhombic unit cell (*6*).

3. Experimental Details

All the samples (x = 0.10, 0.16, 0.20, 0.25, and 0.35) were crushed to a powder, mixed with BN, and pressed into disks containing ~5 mg Fe/cm^2. The Mössbauer equipment was of conventional constant acceleration type utilizing a double-ended vibrator with ^{57}CoRh sources mounted at both ends. One source was used to simultaneously record calibration spectra, using natural iron foils at room temperature as reference absorber.

Mössbauer spectra were recorded in the temperature range 10–300 K using a liquid-helium flow cryostat. In the temperature range 300–950 K a vacuum furnace was utilized.

The recorded spectra were folded and analyzed using a local VAX minicomputer.

4. Results

Representative spectra of $Fe_2P_{1-x}Si_x$ are shown in Figs. 1 and 2. A structural transformation is found to take place in this system with an almost linear temperature dependence vs P/Si substitution, increasing from ~10 K at x = 0.10 to ~825 K at x = 0.35 (Fig. 1 and Table I). This transformation is easily detected by the Mössbauer effect, giving quite different types of spectra.

TABLE I

THE DEPENDENCE OF THE HEXAGONAL/ORTHORHOMBIC TRANSFORMATION TEMPERATURE T_s AND THE CURIE TEMPERATURE T_c ON x IN THE SYSTEM $Fe_2P_{1-x}Si_x$

x	T_s (K)	T_c (K)
0.00	—	216(1)
0.10	≲10	370(5)
0.16	255(10)	450(10)
0.20	340(10)	515(10)
0.25	515(10)	570(10)
0.35	825(25)	660(10)

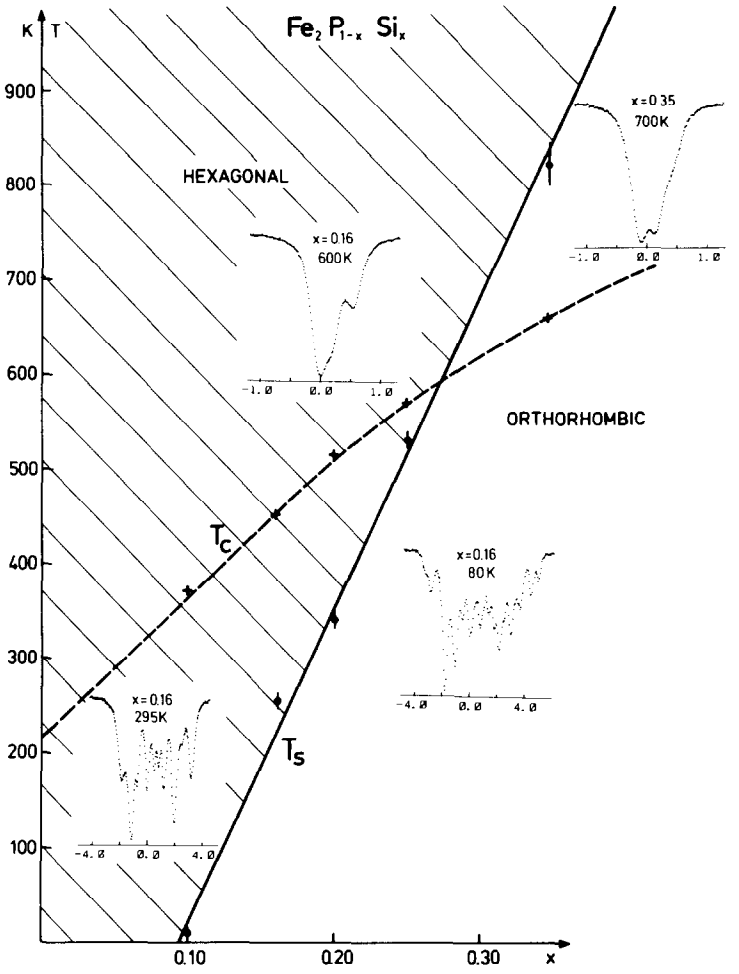

FIG. 1. The hexagonal/orthorhombic transition temperature T_s and the Curie temperature T_c as function of x. Within each phase region a representative spectrum is shown.

It has also been observed by measurements of the magnetic moment as a function of temperature. A weak change in the magnetic anisotropy was observed at the transformation temperature (*7*). The structural transformation was found to take place over a temperature range of ~20 K. From X-ray diffraction measurements it is found that the transformation is between orthorhombic and hexagonal phases (*6*). Furthermore, a magnetic transition is taking place in the system with T_c ranging from ~216 K for $x = 0$ to ~660 K for $x = 0.35$ (Fig. 1 and Table I). The transition for $x = 0$ is of first order (*3*), while for $x > 0$ it seems to be of second order as found also in the other substitution studies. The results for the two structures are presented separately below.

4.1. Hexagonal Phase

In order to determine the type of substitutions, fittings have been made assuming P(1)/Si, P(2)/Si, and random substitutions P/Si for $x = 0.10$, 0.16, and 0.20 when analyzing the spectra in the ferromagnetic re-

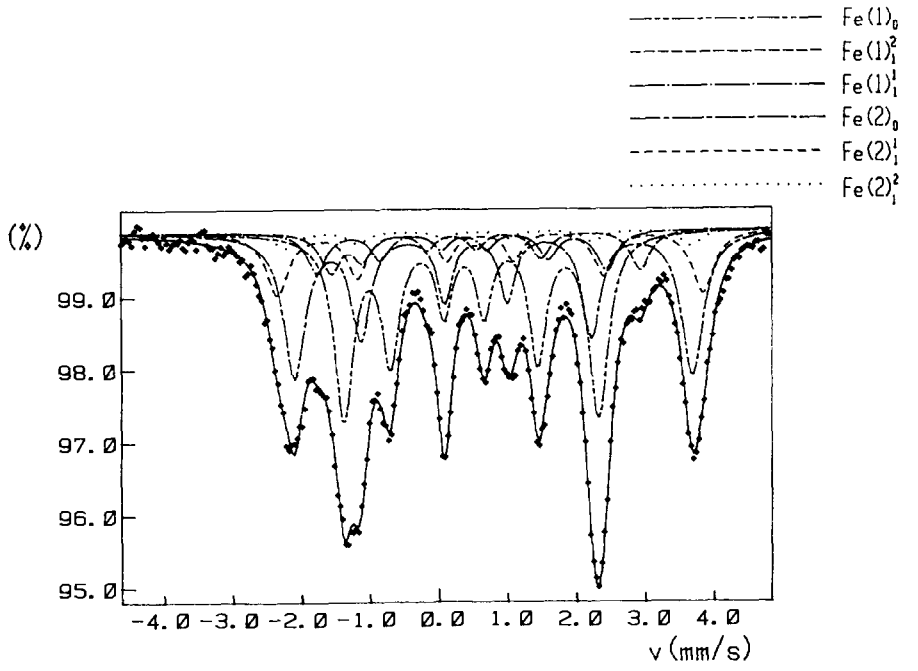

FIG. 2. The experimental and fitted spectrum of $Fe_2P_{0.90}Si_{0.10}$ at 80 K. The decomposition into different iron positions is seen from the broken lines.

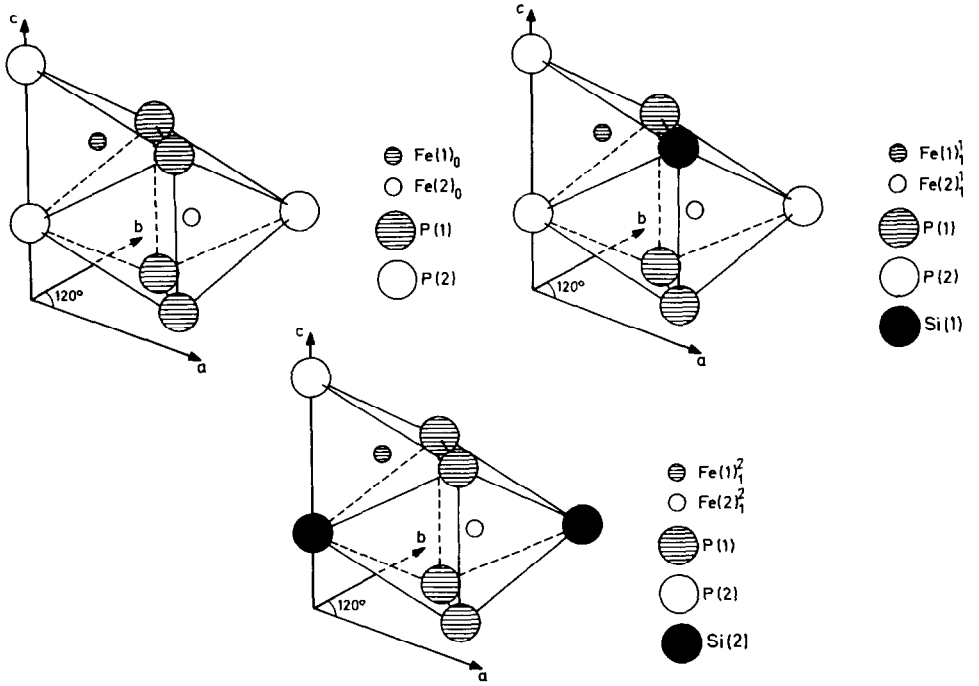

FIG. 3. The six iron positions used in the analysis of the Mössbauer spectra.

gion. In the paramagnetic state the resolution of the spectra is too low to make a detailed analysis.

The iron positions used in the fitting were Fe(1) with no Si neighbor denoted $Fe(1)_0$, Fe(1) with one P(1)/Si substitution denoted $Fe(1)_1^1$, Fe(1) with one P(2)/Si substitution denoted $Fe(1)_1^2$, and the three corresponding Fe(2) positions: $Fe(2)_0$, $Fe(2)_1^1$, and $Fe(2)_1^2$ (Fig. 3). More than one Si neighbor was not considered because of the low probability of the corresponding iron positions. The intensities of the different sets in the Mössbauer spectra were calculated from the coordination numbers, the degrees of substitution and the *f*-factors. For the *f*-factors the Debye temperatures $\theta(Fe(1)) = 383(6)$ K and $\theta(Fe(2)) = 324(9)$ K obtained in the X-ray analysis of Fe_2P (*8*) were used.

The analysis of the spectra assuming random P/Si substitution gives consistent results for all temperatures and substitution levels. It is also possible to fit the spectra one by one assuming P(1)/Si or P(2)/Si substitution. However, in those cases it is not possible to assign any unique set of hyperfine parameters, which could describe all spectra independent of substitution level, to the sites. Furthermore, within one substitution level, the temperature dependence on the hyperfine parameters turns out to be unrealistic, giving large variations of the quadrupole interactions and the isomer shifts, and the ratios between the magnetic hyperfine fields become far from constant.

Using the fitted values of the isomer shifts and assuming that their temperature dependences are pure effects of the second order Doppler shifts, the mean value of the slopes for Fe(1) and Fe(2) gave a rough estimate of the Debye temperatures: $\theta(Fe(1)) \sim 370$ K and $\theta(Fe(2)) \sim 290$ K. The values are in reasonable agreement with the results of the X-ray diffraction analysis, thus supporting the results of the fitting.

Data for $x = 0.10$, $T = 290$ K; $x = 0.16$, $T = 290$ K; and $x = 0.20$, $T = 360$ K are given in Table II, showing the consistency of the hyperfine parameters between different concentrations. The fitted spectrum for $x = 0.10$, $T = 80$ K is presented in Fig. 2, showing the decomposition into different iron positions. Graphs for $x = 0.10$ of the isomer shift δ (linear fit), the quadrupole splitting Δ (linear fit), and the magnetic hyperfine field B (parabolic fit with zero slope at $T = 0$) are given as function of temperature (Fig. 4). Only the three strongest components are plotted but the weaker components give similar plots although with somewhat larger scatter. The ratio between the magnetic hyperfine fields for different positions are almost constant as a function of temperature. The fitted spectra are corrected for the finite thickness of the absorber using algorithms described in detail elsewhere (*9*).

TABLE II

PARAMETERS OBTAINED BY FITTING MÖSSBAUER SPECTRA[a]

	Site	δ (mm/s)	Δ[b] (mm/sec)	B(T)	dB[c] (%)	W (mm/s)	I (%)
$x = 0.10$	$Fe(1)_0$	0.29	0.14	8.86	1.1	0.17	35.7
290 K	$Fe(1)_1^1$	0.25	0.02	10.19	1.1	0.17	7.9
	$Fe(1)_1^2$	0.30	0.43	10.63	1.1	0.17	7.9
	$Fe(2)_0$	0.52	0.25	13.96	1.7	0.15	31.1
	$Fe(2)_1^1$	0.54	0.12	15.20	1.7	0.15	13.8
$\chi^2 = 1.309$	$Fe(2)_1^2$	0.45	0.19	14.19	1.7	0.15	3.5
$x = 0.16$	$Fe(1)_0$	0.30	0.14	9.95	3.3	0.13	30.9
290 K	$Fe(1)_1^1$	0.24	0.03	11.52	3.3	0.13	11.8
	$Fe(1)_1^2$	0.32	0.50	12.11	3.3	0.13	11.8
	$Fe(2)_0$	0.51	0.27	15.51	3.2	0.13	23.3
	$Fe(2)_1^1$	0.51	0.16	16.72	3.2	0.13	15.7
$\chi^2 = 1.531$	$Fe(2)_1^2$	0.48	0.24	15.71	3.2	0.13	4.4
$x = 0.20$	$Fe(1)_0$	0.25	0.13	9.71	5.7	0.13	27.9
360 K	$Fe(1)_1^1$	0.13	0.06	11.23	5.7	0.13	14.0
	$Fe(1)_1^2$	0.30	0.49	11.68	5.7	0.13	14.0
	$Fe(2)_0$	0.46	0.28	14.66	4.1	0.13	19.6
	$Fe(2)_1^1$	0.47	0.15	16.14	4.1	0.13	19.6
$\chi^2 = 1.322$	$Fe(2)_1^2$	0.42	0.26	14.95	4.1	0.13	4.9

Note. The half-width (W) and the field distribution (dB) were constrained to be the same within the iron sites. Estimated accuracy in the fitting values: ±0.01 mm/sec, ±0.03 T, and ±0.3%.

[a] Except for the intensities which were calculated.

[b] The Δ is twice the energy shift of the excited levels due to the quadrupole interaction.

[c] The parameter dB is the half-width of a hyperfine field distribution of Lorenzian shape, relative to the total field.

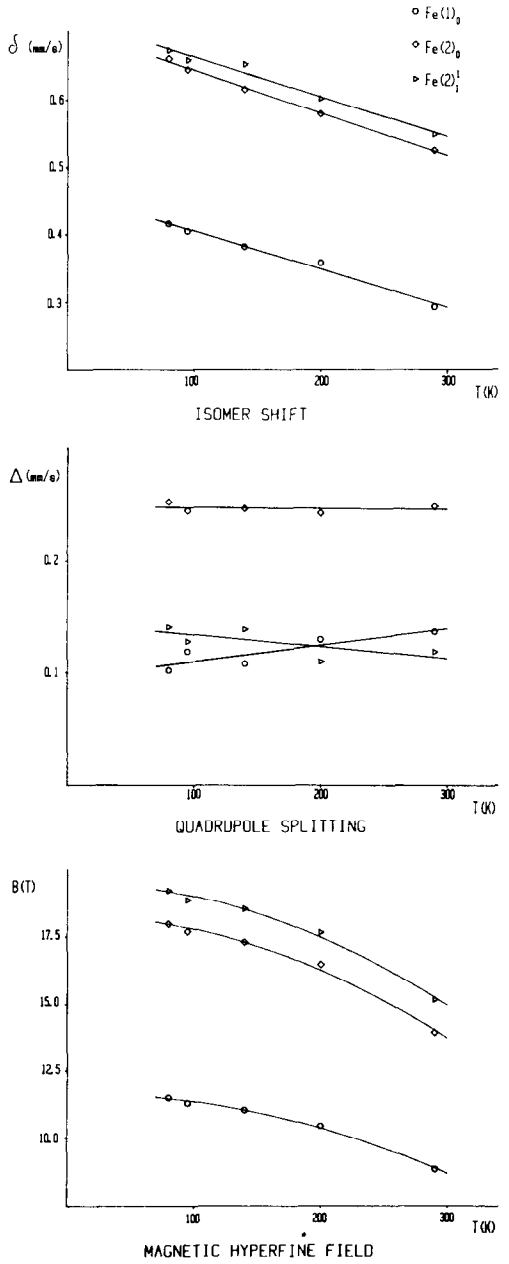

FIG. 4. Hyperfine parameters as function of temperature for $Fe_2P_{0.90}Si_{0.10}$.

4.2. Orthorhombic Phase

The Mössbauer patterns for this phase are complex, especially in the magnetic region, as can be seen in Fig. 1. There exist iron positions where the saturation magnetic hyperfine field are very strong compared to the values in the hexagonal phase (~24 T and ~27 T). According to the Mössbauer spectra, the number of main iron positions are at least six. Furthermore, each main position has several different surroundings due to the P/Si substitution which further increases the number of components in the spectra. A detailed analysis requires a crystal structure refinement and determinations of the magnetic moments, which still are in progress in X-ray and neutron diffraction studies (*6*).

5. Discussion

5.1. The Phase Transformation

In Fig. 5, the relative volume changes, in the hexagonal phase, as a function of x for $Fe_2P_{1-x}As_x$ (data from (*4*)), $Fe_2P_{1-x}Si_x$ (*6*), and $Fe_2P_{1-x}B_x$ (*1*) are plotted. For P/B substitution the cell shrinks while P/As and P/Si substitutions give rise to expansions of the unit cell. As mentioned above, the hexagonal Fe_2P phase was retained upon P/B substitution. This was also reported to be

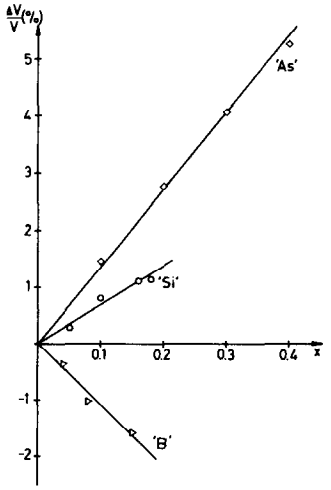

FIG. 5. The relative volume changes as function of x in the systems $Fe_2P_{1-x}B_x$, $Fe_2P_{1-x}Si_x$, and $Fe_2P_{1-x}As_x$.

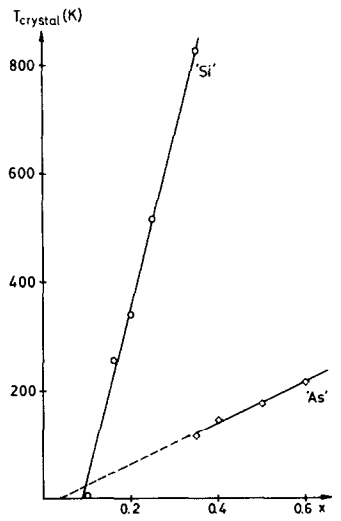

FIG. 6. The structural transformation temperatures as function of x in the systems $Fe_2P_{1-x}Si_x$ and $Fe_2P_{1-x}As_x$.

the case for P/As substitution at room temperature (*4*). In an unreported neutron diffraction study, however, Lundgren (*10*) found a structural transformation for the series $Fe_2P_{1-x}As_x$ at lower temperatures. Those results are presented in Fig. 6. In view of the present results it seems that a structural transformation is likely to take place if the unit cell volume is expanded. From the different slopes of the structural transformation temperature versus x for As and Si substitution, it is clear that the expansion, shown in Fig. 5, cannot be the only driving force for the transformation.

5.2. *The Silicon Substitution*

The recorded Mössbauer spectra can only be explained assuming random (or at least close to random) substitution of Si atoms among the P positions, which is in contradiction to the "size factor" argument which favors preference for a P(1)/Si substitution. However, a slight preference of one of the P positions can still not be excluded from the Mössbauer study, due to its limited sensitivity in this respect.

The tetrahedral covalent radii for P, Si, and As are 1.10, 1.17, and 1.18 Å, respectively (*11*). From (*4*) it is clear that the P/As substitution takes place at the P(1) position. The large difference in the unit cell volume change for P/As and P/Si substitutions in Fe_2P (Fig. 6) indicates that the P/Si substitutions also involve the P(2) position. The relative changes of the c-axis is also quite different for the two kinds of phosphorus substitutions ($\Delta c/c$ $\sim -0.97\%$ for $Fe_2P_{0.90}Si_{0.10}$ (*6*) and $\sim -0.52\%$ for $Fe_2P_{0.90}As_{0.10}$ (*4*)), while the relative changes in the a-axis are about the same (~ 0.91 and 1.02%, respectively).

The different substitution types may be explained using valence electron arguments in addition to the size-factor arguments. The hexagonal phase of Fe_2P, discussed above, may be less stable for substitutions of atoms larger than phosphorus at the P(2) position than at the P(1) position.

5.3. *The Anomalous Cell Axis Behavior*

Possible reasons for the fact that the a-axis is expanding and the c-axis is contracting in the case of P/As, P/Si, and even P/B substitution (*4, 6, 1*), are discussed below, noting that the atomic covalent radii are increasing when going in the sequence B, P, Si, and As (*11*).

The hexagonal Fe_2P phase can be described as arrays of two types of iron tetrakaidecahedra, one irregular and one regular, having a P(1), respectively, a P(2) atom (or their substitutes) located at the centers (Figs. 7 and 8). In the following a simplified model, similar to the one proposed by Rundqvist (*5*), will be used. Both tetrakaidecahedra are assumed to be regular (Fig. 8) and the two types are not distinguished from each other. Furthermore, each tetrakaidecahedron is assumed to be noninteracting with the neighboring tetrakaidecahedra, and to consist of hard spherical atoms. Consider Fig. 8. In the case where the P position is occupied by an P(1)

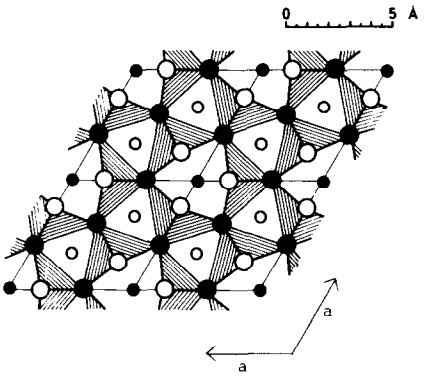

FIG. 7. The structure of Fe_2P projected on (001). ○, Fe(1) ($z = 0$); ●, Fe(2) ($z = \frac{1}{2}$); ○, P(1) ($z = 0$); ●, P(2) ($z = \frac{1}{2}$).

atom (or its substitute), the Fe_I positions are occupied by Fe(2) atoms while the Fe_{II} positions are occupied by Fe(1) atoms. If the P position is occupied by an P(2) atom (or its substitute), the iron atom occupations are reversed. The interatomic distances will be determined by the ratio r/R where r is the effective radius of the central atom (B, P, Si, or As) and R the effective radii of the iron atoms, and by the relative strengths of the bonds between the atoms.

As discussed in (*5*), when $r \sim 0.53R$ each Fe_I atom will be in contact with each of its nearest neighbor iron atoms and with the central atom. Increasing r must then force some of the Fe_I atoms to loose their mutual contact, while the Fe_{II} atoms approach the central atom. At this stage a somewhat different assumption than in (*5*) will be made. In the Fe_2P structure the Fe_I–Fe_I distance in the c-axis direction is far larger than the corresponding distance in the basal plane. It is then reasonable to assume that only the Fe_I–Fe_I distances in the c-axis direction increase when r increases beyond $0.53R$ until a breaking point occur at $r \sim 0.73R$. Above this r-value the Fe_I–Fe_I distance in the basal plane has to increase. At the same time the Fe_I–Fe_I distance in the c-direction will start to decrease keeping the Fe_I–Fe_{II} distance constant. That is to say that the Fe_I–Fe_{II} bonds are stronger than the Fe_I–Fe_I bonds. Assuming the opposite would lead to an expansion of the c-axis with increasing r, which is in contradiction to the experimental results (see below). At $r \sim 0.86R$ another breaking point is reached where the Fe_I–Fe_I distance in the c-axis direction again is equal to $2R$, i.e., the corresponding atoms are in contact as they were for $r \sim 0.53R$.

Using the 12-coordination metallic Goldschmidt radius for iron ~1.27 Å, and the tetrahedral covalent radius for phosphorus ~1.10 Å, as suggested in (*5*), gives $r/R \sim 0.86$. However, the closest Fe–P distance in Fe_2P is 2.22 Å which is 0.15 Å less than $r + R = 2.37$ Å. This suggests in this case to use other values for one or both of the radii. Suppose that it is the covalent phosphorous radius which is too large. Reducing r to 0.95 Å gives $r/R \sim 0.75$, which is reasonable since for phosphorus r/R should fall close to the breaking point where a minimum in the free energy is likely. Far enough from that minimum another structure ought to be more favorable, as found when substituting arsenic (*10*) or silicon to a high level into the phosphorus positions.

Calculations of the relative axes and relative volume changes within this model have been made. Using the tetrahedral covalent

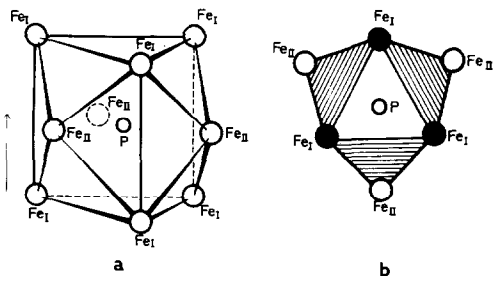

FIG. 8. (a) Tetrakaidecahedral environment of six Fe_I and three Fe_{II} atoms about the central P atom. (b) A tetrakaidecahedron viewed in projection on one of the basal $Fe_IFe_IFe_I$ faces.

radii of B, Si, and As but reduced by the same factor as for P, lead to good qualitative and, within the order of magnitude, to quantitative agreements with experimental results when substituting P with the mentioned elements.

5.4. The Magnetic Transition Temperature

From a simple argument it is proposed and in several cases shown (*12*), that the transition temperature of Fe_2P compounds, perturbed by substitutions, stress, pressure, or iron vacancies, is correlated to a linear combination of the corresponding changes of the unit cell axis: $\Delta a/a - \Delta c/2c$. The correlation holds also for $Fe_2P_{1-x}Si_x$, the values falling very close to the curve (*12*).

5.5. The Isomer Shifts and the Hyperfine Fields

According to the model given by Goodenough (*13*), Fe_2P belongs to a group of transition-metal compounds having only electrons of *d*-character at their Fermi levels. The *p*-band of the anions, located far below the Fermi level, should still be filled on silicon substitutions, i.e., electrons are transferred from the top of the *d*-band to the *p*-band. This implies a decrease of the isomer shift of those iron atoms supplying the electrons, due to a decreased screening of the core *s*-electrons and to an increased valence contribution from the silicon *p*-electrons. Such a decrease was found in the case of Fe(2) with an Si(2) neighbor but not with an Si(1) neighbor. Since a corresponding decrease is, from the same reason, to be expected for iron atoms also on P(1)/Si substitutions, it is reasonable to describe the Fe(1) position with the smaller isomer shift to have an Si(1) neighbor and the other Fe(1) position with almost unchanged isomer shift to have an Si(2) neighbor. That is to say, by this argument, that the electron transfers take place predominantly in the basal planes.

The increase in hyperfine fields can also be explained in this picture since at the top of the *d*-band the density of states of minority spins should be larger than that of the majority spins so that a transfer of electrons from the *d*-band leads to a larger moment. The increased hyperfine fields of those iron atoms that do not supply an electron are then due to the increased Fe–Fe distances leading to a narrower *d*-band and consequently a larger population of the majority spins.

6. Conclusion

A crystallographic phase transition is shown to occur at temperatures depending linearly on the extent of P/Si substitution.

The P/Si substitution is shown to be close to random with respect to the two different phosphorus sites. A more accurate estimate may be obtained from EXAFS spectra measured at the K-edge of phosphorus using Fe_2P and $Fe_2P_{1-x}B_x$ or $Fe_2P_{1-x}As_x$, in which one kind of the substitutions is strongly preferred, as reference materials.

The magnetic ordering temperature is shown to increase with increasing substitution.

The magnetic hyperfine fields are shown to increase for iron atoms having one silicon neighbor which can be explained by increasing moments due to electron transfer and narrowing of the *d*-band.

Acknowledgments

The authors are very grateful to Dr. Leif Lundgren, Institute of Technology, Uppsala, for making available his results prior to publication.

References

1. R. CHANDRA, S. BJARMAN, T. ERICSSON, L. HÄGGSTRÖM, C. WILKINSON, AND R. WÄPPLING, *J. Solid State Chem.* **34,** 389 (1980).
2. T. ERICSSON, L. HÄGGSTRÖM, R. WÄPPLING, AND T. METHASIRI, *Phys. Scrip.* **21,** 212 (1980).

3. R. WÄPPLING, L. HÄGGSTRÖM, T. ERICSSON, S. DEVANARAYANAN, E. KARLSSON, B. CARLSSON, AND S. RUNDQVIST, *J. Solid State Chem.* **13,** 258 (1975).
4. A. CATALANO, R. J. ARNOTT, AND A. WOLD, *J. Solid State Chem.* **7,** 262 (1973).
5. S. RUNDQVIST, *Ark. Kemi* **20,** 67 (1962).
6. Y. ANDERSSON, in press.
7. L. LUNDGREN, P. NORDBLAD, O. BECKMAN, in press.
8. B. CARLSSON, M. GÖLIN, AND S. RUNDQVIST, *J. Solid State Chem.* **8,** 57 (1973).
9. P. JERNBERG, *Nucl. Instrum. Methods B,* in press.
10. L. LUNDGREN, Institute of Technology, Uppsala University, Box 534, 751 21 Uppsala, Sweden (private communication).
11. L. PAULING, "Nature of the Chemical Bond," 2nd ed., p. 179, Cornell Univ. Press, Ithaca, N.Y. (1960).
12. L. LUNDGREN, P. NORDBLAD, AND O. BECKMAN, UPTEC 8014 R, Institute of Technology, Uppsala University, Box 534, Sweden (1980).
13. J. B. GOODENOUGH, *J. Solid State Chem.* **7,** 428 (1973).